Performance of Concatenated Optimized Irregular LDPC Code with Alamouti Coded MIMO-OFDM Systems

Bhasker Gupta and Davinder S. Saini
Department of Electronics and Communication
Jaypee University of Information Technology, Waknaghat, Solan, H.P., INDIA-173234
e-mail: guptabhasker@jieee.org and davinder.saini@juit.ac.in

Abstract: -Multiple input multiple output (MIMO) communication systems along with orthogonal frequency division multiplexing (OFDM) have a great potential for future 4G broadband wireless communications. Recently, low density parity check codes (LDPC) achieves good error correcting performance and capacity near Shannon's limit. In this paper, we considered the performance analysis of serially concatenated regular and irregular LDPC codes with Alamouti space time block coded (STBC) and space frequency block coded (SFBC) MIMO-OFDM systems for high data rate wireless transmission. Currently, most of the research related to this area is concentrated on the impact of increase in code rate and diversity of the system but not on increase in coding gain. In this paper, we analyzed the impact of increasing coding gain. Performance analysis and design optimization is carried out using density evolution (DE) tool with mixture of Gaussian approximations over Rayleigh independent and identically distributed (i.i.d) channels

Key-Words: - MIMO-OFDM, Alamouti codes, Density Evolution (DE), LDPC codes, Maximum a Posteriori (MAP), Maximum Likelihood (ML) detection.

1 Introduction

The key features of next generation systems like 4G is to provide high system capacity, high voice quality and high data rate in all practical environments like macro and micro, rural, sub-urban and urban, indoor and outdoor. To achieve above goals, MIMO [1-4] antenna systems are used recently. MIMO systems are not only bandwidth efficient but they also provide improved system reliability through diversity as well as data rate increase though spatial multiplexing. In wireless environments, when signal propagates through multiple paths, it gets attenuated and delayed leading to multipath fading. Multipath fading is a major constrained in any wireless system performance degradation. To combat fading, the signal is propagated through multiple independent fading paths in time, frequency or space domains and combined constructively at the receiver. This results in time, frequency and space diversities. In order to take diversity advantage, a number of space time (ST) ([5]-[7]), space frequency (SF) ([8]-[9]) and space time frequency STF) ([10]-[12]) codes are proposed in narrowband and broadband wireless communication systems. In ST coding, full diversity is defined as product of number of transmit (M_T) and receive (M_R) antennas i.e. M_TM_R, whereas in SF and STF it is equal to M_TM_RL and $M_TM_RN_bL$ [13] respectively in frequency selective block fading MIMO channels, where L and N_b are number of delay paths and number of fading blocks. In broadband communication systems, frequency diversity is explored by combining MIMO with OFDM [14] because it will transform frequency selective channels into set of parallel frequency flat channels. OFDM [14] helps to mitigate fading as well as inter symbol interference (ISI). Further, ISI can be reduced by adding cyclic prefix (CP) to each OFDM symbol.

In MIMO-OFDM systems, research mainly focused on designing ST, SF and STF codes which can achieve full rate with full diversity and with minimal decoding complexity. Recently in [13], work is reported on designing high rate STF codes with full diversity and minimum decoder complexity. Decoder complexity can be further reduced by employing some modified or novel equalizers mentioned in ([15]-[20]). MIMO-OFDM systems are employed in next generation wireless local area networks (WLAN) to achieve data rate more than 100Mb/s, which is at par with wired Ethernet technology. To further improve robustness and feasibility, coding gain benefit can be added by concatenating MIMO-OFDM systems with error correcting codes. Convolutional codes (CC) ([21]-[22]), turbo codes ([22]-[23] and LDPC codes ([24]-[27]) are used for concatenation as mentioned in IEEE 802.11a/g. However, CC codes are not preferred these days due to their large capacity gap with respect to Shannon's limit [24]. LDPC codes can be used in conjunction with MIMO-OFDM

systems to bridge the capacity gap. LDPC codes provide design flexibility and performance tradeoff in terms of complexity. Thus, LDPC codes turns out be solution for next generation WLAN systems such as IEEE 802.11n.

In this paper, we analyzed the performance of concatenated LDPC codes with Alamouti coded [6] MIMO-OFDM systems. The performance is analyzed using DE ([28]-[29]) techniques under Rayleigh frequency flat channels mentioned in digital video broadcast-next generation handheld (DVB-NGH) standard [30]. DE tool is used to estimate probability density function (pdf) of information (LLR form) passed between check nodes and bit nodes of Tanner graph [31] (used during decoding process). The pdf's are function of SNR as well as iteration number and is used for probability of error computation after every iteration. The conventional iterative receiver [26] used to decode above system consists of MAP soft input soft output decoder called soft demapper along with LDPC decoder ([32]-[33]). The mentioned iterative receiver suffers from higher computational complexity as compared to CC (Viterbi receiver). Efforts are made to reduce this decoder complexity by using bypass decoder [34] and semi iterative receiver [35] in AWGN and Rayleigh channels [36]. In this paper, we are combining optimized LDPC codes with Alamouti ST and SF codes in order to take diversity advantage along with reduced decoder complexity. The decoder complexity is reduced due to linear combination of receiver estimates by ML method as suggested by Alamouti. BER results are compared with existing results in terms of number of errors, SNR_{min-op} and complexity issues. SNR_{min-op} [26] is defined as minimum operational signal to noise ratio (SNR) required for which probability of error tends to zero.

The rest of the paper is organized as follows. In section 2 and 3, we described the transmitter and receiver structure of LDPC coded Alamouti MIMO-OFDM systems with brief encoding and decoding schemes summary.

In section 4, we discussed how to analyze and optimize LDPC codes with and without Alamouti coding. In section 5, different simulation results are presented with Alamouti STBC and SFBC schemes concatenated with regular and irregular LDPC codes in different MIMO system configurations. The paper is concluded in section 6.

2 Transmitter Description

The generalized schematic of LDPC coded $M_T \times M_R$ Alamouti MIMO-OFDM system is shown in Fig. 1, Initially, a block of k bits of incoming data stream is encoded by a rate r = k/n regular or ire gular LDPC code. The LDPC encoding is done to introduce redundancy in original information, which enables the receiver to correct errors. The resultant n coded bits are mapped into data symbols via M-PSK modulation technique, which leads to block of $n / \log_2 M$ symbols, where M is constellation size. In each OFDM time slot, only $N_C M_T$ out of $n/\log_2 M$ symbols can be transmitted simultaneously through N_C OFDM subcarriers and M_T transmitting antennas. This would results into $(n/\log_2 M)/N_C M_T$ = T OFDM time slots.

To achieve high diversity performance, data symbols are further encoded by Alamouti STBC and SFBC transmit diversity scheme. OFDM symbols are produced by transforming frequency domain signals to time domain by applying inverse fast Fourier transform (IFFT). CP is then appended on each OFDM block whose length is considered to be longer than channel delay spread. These symbols are transmitted simultaneously through M_T transmitting antennas. The information is then passed through Rayleigh i.i.d. channel that has been generated based upon digital video broadcast (DVB)-next generation handheld (NGH) standard [30].

2.1 Low Density Parity Check (LDPC) Encoding

LDPC codes are linear error correcting block codes which are characterized by its very sparse parity check matrix ***H***.

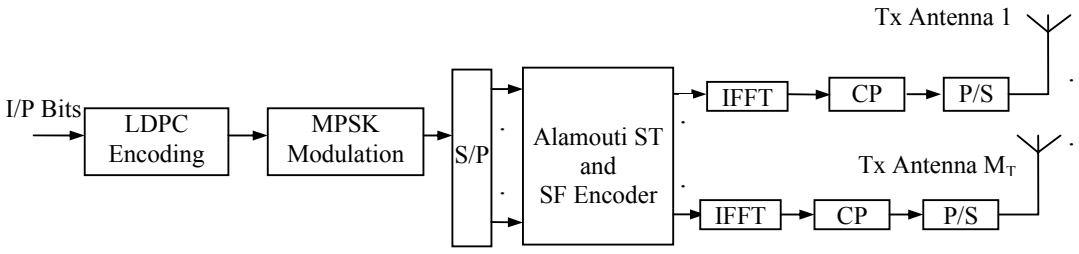

Fig. 1 Concatenated LDPC with Alamouti coded MIMO-OFDM transmitter structure

These codes are generally called capacity approaching codes because system capacity using these codes is close to Shannon's capacity limits [24]. An LDPC code is denoted as C_{LDPC} (n, k, s, t), where n and k are number of output and input bits with number of '1's in each column and t number of '1's in each row. Usually t>s and s<< n, the '1's are placed at random positions in a parity check matrix of size (n-k)×n. These codes are of two types namely regular and irregular depending upon whether number of '1's per row per column is fixed or varying.

LDPC encoding algorithm can be represented by bipartite graph called Tanner graph [31] as shown in Fig. 2, it consists of two types of nodes, the symbol nodes or variable nodes d_j, which represents transmitted symbols or bits and the parity check nodes h_i, which represents each row of parity check matrix. If $\boldsymbol{H}_{i,j}$=1, it means an edge is placed between variable node d_j and check node h_i. In regular LDPC codes, all nodes of same type will have same degree profile. For irregular LDPC codes, degrees of each set of nodes are chosen according to some distribution. Thus, irregular LDPC codes are characterized by two polynomials as shown below.

$$\lambda(x)=\sum_{i=1}^{d_v}\lambda_i x^{i-1} \quad (1)$$

$$\rho(x)=\sum_{i=1}^{d_c}\rho_i x^{i-1} \quad (2)$$

Where, λ_i is fraction of edges in bipartite graph that are connected to variable nodes of degree i and ρ_i is the fraction of edges in the same graph that are connected to check nodes of degree i. Identifiers d_v and d_c are maximum degrees of variable nodes and check nodes respectively.

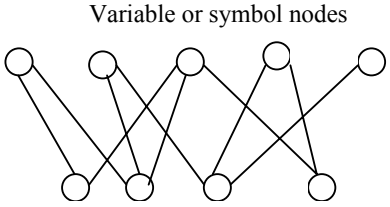

Fig. 2 Tanner graph showing symbol and check nodes

2.2 Alamouti Coding

The input block size of $N_C T \times M_T$ in T OFDM slots are encoded into codeword matrix as shown below.

$$\mathbf{C}_{ST}=\begin{bmatrix} c_{1,1} & c_{1,2} & \dots & c_{1,M_T} \\ c_{2,1} & c_{2,2} & \dots & c_{2,M_T} \\ \dots & \dots & \dots & \dots \\ c_{T,1} & c_{T,2} & \dots & c_{T,M_T} \end{bmatrix} \in \mathbf{C}^{N_C T \times M_T} \quad (3)$$

The codeword matrix $\mathbf{C}_{ST}$ in (3) encodes the data symbols in Space-Time (ST) domain [9]. It can be modified to form Space-Frequency (SF) codeword matrix $\mathbf{C}_{SF}$ as given below.

$$\mathbf{C}_{SF}=\begin{bmatrix} c_1(0) & c_2(0) & .. & c_{M_T}(0) \\ c_1(1) & c_2(1) & .. & c_{M_T}(1) \\ \dots & \dots & .. & .. \\ c_1(N_c-1) & c_2(N_c-1) & .. & c_{M_T}(N_c-1) \end{bmatrix} (4)$$

Each element $c_i(j)$ of matrix (4) represents data symbol transmitted through mentioned transmitting antenna and subcarrier. Alamouti proposed orthogonal STBC [6] design for 2×1 and 2×2 MIMO systems to achieve high diversity performance with low decoding complexity. According to Alamouti scheme, at a particular time instant two symbols can be simultaneously transmitted from the two antennas. Let the symbols transmitted from antenna 1 and 2 are x_1 and x_2 during time instant t and $-x_2^*$ and x_1^* during next time instant t+T, where * is the complex conjugate operation. This scheme is shown in Table 1.

Table 1. Alamouti space time (ST) encoding scheme

	Transmitter antenna 1	Transmitter antenna 2
Time (t)	x_1	x_2
Time (t+T)	$-x_2^*$	x_1^*

Where, each row and column of above Table indicates time and space. An Alamouti code achieves diversity of 2 and code rate 1 with low decoding complexity. To increase more reliability, Alamouti code can be extended to SF domain as shown in Table 2.

Table 2. Alamouti space frequency (SF) encoding scheme

	OFDM-Subcarrier	
	K	L
Transmitting antenna 1	x_1	$-x_2^*$
Transmitting antenna 2	x_2	x_1^*

Table 2, shows two symbols x_1 and $-x_2^*$ are transmitted from subcarriers K and L of one OFDM block and through antenna 1. Similarly symbols x_2 and x_1^* are transmitted from subcarriers K and L of same OFDM block but through antenna 2. Using above code diversity is increased, but not always as it happened in frequency selective channel.

3 Schematic of iterative receiver structure

After passing the information through Rayleigh i.i.d channel, receiver removes the CP and applies FFT on frequency tones as shown in Fig. 3, Afterwards, it is fed to Alamouti decoder and then mapped to turbo iterative receiver which consists of soft input soft output MAP demodulator [26] (soft demodulator) and LDPC decoder.

3.1 Alamouti Decoding with One and Two Receive Antenna

According to Alamouti STBC [6], the received signals with two transmit and one receive antenna can be represented by

$$y_1 = y(t) = h_1 x_1 + h_2 x_2 + n_1 \quad (5)$$

$$y_1 = y(t) = h_1 x_1 + h_2 x_2 + n_1 \quad (6)$$

Where, y_1 and y_2 are received signals at time t and t+T. h_1 and h_2 channel coefficients between particular receiver and transmitter antenna pair. n_1 and n_2 are Gaussian random variables with mean zero and variance σ^2. Receiver estimates of transmitted symbols x_1 and x_2 are given by

$$\hat{x}_1 = h_1^* y_1 + h_2 y_2^* = \left(\alpha_1^2 + \alpha_2^2\right) x_1 + h_1^* n_1 + h_2 n_2^* \quad (7)$$

$$\hat{x}_2 = h_2^* y_1 - h_1 y_2^* = \left(\alpha_1^2 + \alpha_2^2\right) x_1 - h_1^* n_1 + h_2 n_2^* \quad (8)$$

Where, α_1 and α_2 are channel amplitudes or gains for h_1 and h_2. The transmitted signals are obtained from their receiver estimates by applying ML detection algorithm on it. In above case, ML detection amounts to minimizing the following decision metric over all possible values of x_1 and x_2.

$$\left|y_1 - \alpha_1 x_1 - \alpha_2 x_2\right|^2 + \left|y_2 + \alpha_1 x_2^* - \alpha_2 x_1^*\right|^2 \quad (9)$$

Decoding scheme in (9) requires full search over all possible pairs of x_1 and x_2 and its complexity grows exponentially with increase in number of transmitting antennas. Expanding and deleting terms that are independent of codewords, the above minimization problem can be decomposed into two parts for separately decoding x_1 and x_2 is shown below.

$$\left|x_1\right|^2 \left[\left(y_1 \alpha_1^* + y_2^* \alpha_2 - x_1\right)^2 + \left(\alpha_1^2 + \alpha_2^2 - 1\right)\right] \quad (10)$$

$$\left|x_2\right|^2 \left[\left(y_1 \alpha_2^* - y_2^* \alpha_1 - x_2\right)^2 + \left(\alpha_1^2 + \alpha_2^2 - 1\right)\right] \quad (11)$$

Above decomposition will reduce the decoder complexity, it will now increase linearly instead of exponentially with increase of number of transmitting antennas. Alamouti received signals with 2 transmit and 2 receive antennas can be represented as follows

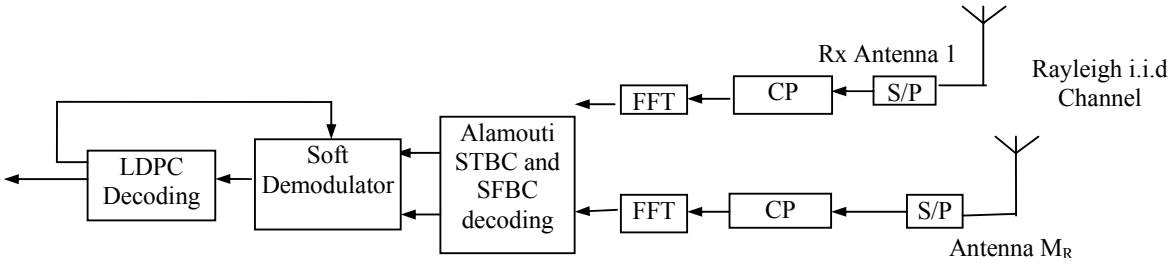

Fig 3, Turbo receiver structure for LDPC coded MIMO-OFDM system

$$\begin{aligned} y_{11} &= y_1(t) = h_{11} x_1 + h_{21} x_2 + n_{11} \\ y_{12} &= y_1(t+T) = -h_{11} x_2^* + h_{21} x_1^* + n_{12} \\ y_{21} &= y_2(t) = h_{12} x_1 + h_{22} x_2 + n_{21} \\ y_{22} &= y_2(t+T) = -h_{12} x_2^* + h_{22} x_1^* + n_{22} \end{aligned} \quad (12)$$

Where, $y_j(t)$ represents received signal at j^{th} receiving antenna, $h_{i,j}(t)$ is channel coefficient between i^{th} transmit antenna and j^{th} receive antenna and $n_{i,j}$ is Gaussian noise of zero mean and σ^2. variance. Receiver estimates of transmitted

symbols x_1 and x_2 with two receivers are given as

$$\hat{x}_1 = h_{11}^* y_{11} + h_{12}^* y_{21} + h_{21} y_{12}^* + h_{22} y_{22}^*$$
$$\hat{x}_1 = \left(\alpha_{11}^2 + \alpha_{21}^2 + \alpha_{12}^2 + \alpha_{22}^2\right)x_1 + h_{11}^* n_{11} + h_{21} n_{12}^* + h_{12}^* n_{21} + h_{22} n_{22}^* \quad (13)$$

$$\hat{x}_2 = h_{21}^* y_{11} - h_{11} y_{12}^* + h_{22}^* y_{21} - h_{12} y_{22}^*$$
$$= \left(\alpha_{11}^2 + \alpha_{21}^2 + \alpha_{12}^2 + \alpha_{22}^2\right)x_2 - h_{11} n_{12}^* + h_{21}^* n_{11} - h_{12} n_{22}^* + h_{22}^* n_{21} \quad (14)$$

Further, ML detection is applied to decode x_1 and x_2 as we done in (9), (10) and (11). Similarly, whole process can be repeated for Alamouti SFBC.

3.2 Iterative Receiver

Output of Alamouti decoder is translated or mapped to soft demodulator. A serial concatenated turbo iterative receiver is then employed which consists of combination of soft demodulator and LDPC decoder. Iterative receiver is based on passing extrinsic information between soft demodulator and LDPC decoder. Extrinsic information is in log likelihood ratio (LLR) form which is denoted by L. This information is iteratively passed along the edges in the bipartite graph during p^{th} round of inner iteration within LDPC decoder and qth round of outer iteration between the LDPC decoder and soft demodulator. The extrinsic information of LDPC coded bit (b_i) is given as

$$L^{q}_{S.De\,mod\to L.Dec}\left(b_{i,j}\right) = \log\frac{P\left(b_{i,j}=+1/\mathbf{y}\right)}{P\left(b_{i,j}=-1/\mathbf{y}\right)} - L^{q-1}_{S.De\,mod\leftarrow L.Dec}\left(b_{i,j}\right) \quad (15)$$

Where, $L^{q}_{S.De\,mod\to L.Dec}$ is extrinsic information sent from soft demodulator to LDPC decoder during q^{th} iteration and $L^{q-1}_{S.De\,mod\leftarrow L.Dec}\left(b_{i,j}\right)$ is sent from LDPC decoder to soft demodulator during previous $(q-1)^{th}$ iteration assuming it to be zero at first turbo iteration, **y** is received signal matrix which contains signals from all receiving antennas i.e. $\mathbf{y}=[y_1, y_2, \ldots, y_{M_R}]$. For a particular subcarrier and time slot, total $M_T \log_2 M$ bits are transmitted from M_T antennas. Thus, $L^{q}_{S.De\,mod\to L.Dec}$ is computed for i=1,2,……., $M_T \log_2 M$ bits as shown below.

$$L^{q}_{S.De\,mod\to L.Dec}\left(b_{i,j}\right) = \log\frac{\sum_{\mathbf{x}^+\in C_i^+} P\left(\mathbf{x}=\mathbf{x}^+/\mathbf{y}\right)}{\sum_{\mathbf{x}^-\in C_i^-} P\left(\mathbf{x}=\mathbf{x}^-/\mathbf{y}\right)} - L^{q-1}_{S.De\,mod\leftarrow L.Dec}\left(b_{i,j}\right) \quad (16)$$

Where, c_i^+ and c_i^- are set of values of **x** (transmission matrix for M_T transmitting antenna) for which LDPC coded bit is +1or -1. In a MAP MIMO-OFDM demodulator, (16) can be rewritten as

$$L^{q}_{S.De\,mod\to L.Dec}\left(b_{i,j}\right) = \log\frac{\sum_{\mathbf{x}^+\in C_i^+} P\left(\mathbf{y}/\mathbf{x}=\mathbf{x}^+\right)P\left(\mathbf{x}=\mathbf{x}^+\right)}{\sum_{\mathbf{x}^-\in C_i^-} P\left(\mathbf{y}/\mathbf{x}=\mathbf{x}^-\right)P\left(\mathbf{x}=\mathbf{x}^-\right)} - L^{q-1}_{S.De\,mod\leftarrow L.Dec}\left(b_{i,j}\right) \quad (17)$$

$$= \log\frac{\sum_{\mathbf{x}^+\in C_i^+}\exp\left(-\left\|\mathbf{y}-\sqrt{\frac{SNR}{N_o}}\mathbf{H}\mathbf{x}^+\right\|^2 + \sum_{j=1}^{M_T\log_2(M)} x_j^+ \frac{L^{q-1}_{S.Demod\leftarrow L.Ded}\left(b_{k,j}\right)}{2}\right)}{\sum_{\mathbf{x}^-\in C_i^-}\exp\left(-\left\|\mathbf{y}-\sqrt{\frac{SNR}{N_o}}\mathbf{H}\mathbf{x}^-\right\|^2 + \sum_{j=1}^{M_T\log_2(M)} x_j^- \frac{L^{q-1}_{S.Demod\leftarrow L.Ded}\left(b_{k,j}\right)}{2}\right)} - L^{q-1}_{S.Demod\leftarrow L.Ded}\left(b_{i,j}\right) \quad (18)$$

Where, **H** is channel frequency response matrix and $\mathbf{x}_j^+, \mathbf{x}_j^-$ represents j^{th} bit in symbol $\mathbf{x}^+$ and $\mathbf{x}^-$.The message passing or belief propagation [32] method is used to describe inner iterations within LDPC decoder. Message passing between variable and check nodes are described using LLR's which is denoted as $L^{p,q}_{d\to h}\left(\ell^{d}_{i,m}\right)$, where $d \to h$ represents quantities passed from variable node to check nodes of the LDPC code and vice versa. Thus, $L^{p,q}_{d\to h}\left(\ell^{d}_{i,m}\right)$ denotes extrinsic message passed from variable node to check node along m^{th} edge connected to i^{th} variable node during p^{th} iteration within LDPC decoder and q^{th} iteration between LDPC decoder and soft demodulator. The message passing algorithm consists of following steps.

3.2.1 Updating variable and check nodes

LLR's passed in-between variable nodes and check nodes are updated with every iteration. These can be represented as follows.

$$L^{p,q}_{d\to h}\left(\ell^{d}_{i,m}\right) = L^{q}_{S.De\,mod\to L.Dec}\left(b_i\right) + \sum_{k=1,k\neq m}^{\deg(d_j)} L^{p-1,q}_{d\leftarrow h}\left(\ell^{d}_{i,k}\right) \quad (19)$$

$$L^{p,q}_{d\leftarrow h}\left(\ell^{h}_{i,m}\right) = 2\tanh^{-1}\left[\prod_{k=1,k\neq m}^{\deg(h_i)}\tanh\left(\frac{L^{p,q}_{d\to h}\left(\ell^{h}_{i,k}\right)}{2}\right)\right] \quad (20)$$

3.2.2 Compute extrinsic messages

Based upon above updates extrinsic messages are computed and then sent back from LDPC decoder to soft demodulator as shown below.

$$L^{q}_{S.De\,mod\leftarrow L.Dec}(b_i) = \sum_{k=1}^{\deg(d_j)} L^{p,q}_{d\leftarrow h}\left(\ell^{d}_{i,k}\right) \quad (21)$$

3.2.3 Store LLR's for next iteration

Inner iterative LLR, calculated in (21) can be stored and used as basis for next outer iteration.

$$L^{0,q+1}_{d\leftarrow h}\left(\ell^{d}_{i,k}\right) = L^{p,q}_{d\leftarrow h}\left(\ell^{d}_{i,k}\right) \quad (22)$$

3.2.4 Hard decision decoding

At last, hard decisions are made for information and parity bits but after sufficient Q turbo iterations are shown as under

$$\hat{b}_i = \text{sign}\left[L^{Q}_{S.De\,mod\rightarrow L.Dec}(b_i) + L^{Q}_{S.De\,mod\leftarrow L.Dec}(b_i)\right] \quad (23)$$

4 Density Evolution (DE) analysis for LDPC codes

In this section, we use DE ([28]-[29]) as a tool for analyzing system performance which is based on computing average probability of incorrect bits. This can be done by estimating the probability density function (pdf) of extrinsic messages passed between variable nodes and check nodes during each iteration of decoding algorithm. When the number of codewords is infinite, then extrinsic information between each variable and check nodes considered to be independent random variables. Initially, LLR from variable node to check node is given by $L^{0,0}_{d\rightarrow h}(b_i) = \frac{2}{\sigma^2}\mathbf{y}$ and its pdf for Rayleigh i.i.d channel can be represented as

$$f^{0,0}_{d\rightarrow h}(x) = \frac{x}{4/\sigma^2} e^{\frac{-x^2}{2(4/\sigma^2)}} \quad (24)$$

The distribution in (24) represents Rayleigh distribution with mean $\sigma\sqrt{\frac{\pi}{2}}$ and variance $\frac{4-\pi}{2}\left(\frac{4}{\sigma^2}\right)$. For regular LDPC codes, the pdf's from variable nodes to check nodes and vice versa after p^{th} inner and q^{th} outer iterations are given by [25].

$$f^{p,q}_{d\rightarrow h}(x) = f^{0,0}_{d\rightarrow h}(x) \otimes \left(f^{p,q}_{d\leftarrow h}(x)\right)^{\otimes(d_v-1)} \quad (25)$$

$$f^{p,q}_{d\leftarrow h}(x) = \Gamma^{-1}\left(\left(\Gamma\left(f^{p-1,q}_{d\rightarrow h}(x)\right)\right)^{\otimes(d_c-1)}\right) \quad (26)$$

Where, $\otimes$ stands for convolution operator and Γ is probability transformation function generated from other function $\gamma(x) \in GF(2)\times[0,+\infty]$, which is given as

$$\gamma(x) = \left(\text{sgn}(x), -\ln\tanh\left|\frac{x}{2}\right|\right) \quad (27)$$

Where, sgn(x)=0 if x≥0 and sgn(x)=1 if x<1, GF(2) is Galois or finite field of two elements which are nearly 0 and 1.Thus, the average probability of error after p inner and q outer iterations can be defined as

$$P^{p,q}_{e}(x) = \int_{-\infty}^{0} f^{p,q}_{d\rightarrow h}(x)dx \quad (28)$$

The expressions in (25) and (26) can be extended for irregular LDPC codes as follows.

$$f^{p,q}_{d\rightarrow h}(x) = f^{0,0}_{d\rightarrow h}(x) \otimes \sum_{i\geq 2}\lambda_i\left(f^{p,q}_{d\leftarrow h}(x)\right)^{\otimes(i-1)} \quad (29)$$

$$f^{p,q}_{d\leftarrow h}(x) = \Gamma^{-1}\left(\sum_{i\geq 2}\left(\Gamma\left(f^{p-1,q}_{d\rightarrow h}(x)\right)\right)^{\otimes(i-1)}\right) \quad (30)$$

The expression of probability of error for irregular codes will be similar to (28). To explore DE for Alamouti coded LDPC codes, we have to derive pdf of initial LLR and then pdf after p inner and q outer iterations.

4.1 Alamouti Coded LDPC with Two Transmitting and One Receiving Antennas

In this section, the pdf for concatenation of Alamouti coding with LDPC codes in Rayleigh i.i.d channels is presented. From (7) we have

$$\begin{aligned} y = \hat{x}_1 &= h_1^* y_1 + h_2 y_2^* = \left(\alpha_1^2+\alpha_2^2\right)x_1 + h_1^* n_1 + h_2 n_2^* \\ &= \left(\alpha_1^2+\alpha_2^2\right)x + \alpha_1 n_1' + \alpha_2 n_2' \end{aligned} \quad (31)$$

Where, n_1' and n_2' are Gaussian random variables with mean 0 and variance σ^2 .Let $\alpha = \alpha_1^2+\alpha_2^2$, then y can be represented as Gaussian variable with mean α and variance $\alpha\sigma^2$ The input to LDPC decoder at time t+T will yield same result as of (31).Thus, pdf of y and its initial LLR is given by

$$f(y/x,\alpha)=\frac{1}{\sqrt{2\pi\alpha\sigma^2}}e^{\frac{-(y-\alpha x)^2}{2\alpha\sigma^2}} \quad (32)$$

$$L_{d\to h}^{0,0}(b_i)=\ln\frac{p(y/x=1,\alpha)}{p(y/x=-1,\alpha)}=\frac{2}{\sigma^2}y \quad (33)$$

Equation (33) indicates that initial LLR is a Gaussian random variable with mean $\frac{2\alpha}{\sigma^2}$ and variance $\frac{4\alpha}{\sigma^2}$. To compute pdf of initial LLR, we need to derive pdf of α. We considered Rayleigh i.i.d. channel, so α_1 and α_2 can be represented by $\alpha_1=X_1^2+X_2^2$ and $\alpha_2=X_3^2+X_4^2$, collectively it can be represented by.

$$\alpha=\sum_{i=1}^{4}X_i^2 \quad (34)$$

Where, X is Gaussain random variable with mean 0 and variance 1/2.Thus, pdf of α for m such samples is given as

$$f(\alpha)=\frac{1}{\sigma^m 2^{m/2}\Gamma_f\left(\frac{m}{2}\right)}\alpha^{m/2-1}e^{\left(-\alpha/2\sigma^2\right)} \quad (35)$$

Where, Γ_f is a Gamma function. Put m=4 in (35), then pdf of α is given as $f(\alpha)=\alpha e^{-\alpha}$. Finally, pdf of initial LLR is given by

$$f_{d\to h}^{0,0}(x)=\int_0^\infty\frac{1}{\sqrt{2\pi\left(4\alpha/\sigma^2\right)}}e^{\frac{-\left(x-2\alpha/\sigma^2\right)^2}{8\alpha/\sigma^2}}\alpha e^{-\alpha}d\alpha \quad (36)$$

At last pdf after p inner and q outer iterations are obtained by using (29) and (30).

4.2 Alamouti Coded LDPC with Two Transmitting and Two Receiving Antennas

In this section, we presented the pdf for concatenation of Alamouti coding with LDPC codes with two transmitting and two receiving antennas. From (13) we have

$$\begin{aligned}y=\hat{x}_1&=\left(\alpha_{11}^2+\alpha_{21}^2+\alpha_{12}^2+\alpha_{22}^2\right)x_1+h_{11}^*n_{11}+h_{21}n_{12}^*+h_{12}^*n_{21}+h_{22}n_{22}^*\\&=\left(\alpha_{11}^2+\alpha_{21}^2+\alpha_{12}^2+\alpha_{22}^2\right)x+\alpha_{11}n'_{11}+\alpha_{21}n'_{12}+\alpha_{12}n'_{21}+\alpha_{22}n'_{22}\end{aligned} \quad (37)$$

Where, $n'_{11}, n'_{12}, n'_{21}$ and n'_{22} are Gaussian random variables with mean 0 and variance σ^2. Similar to section 4.1, let $\beta=\left|\alpha_{11}^2+\alpha_{12}^2+\alpha_{21}^2+\alpha_{22}^2\right|$, it means y will be Gaussian variable with mean β and variance $\beta\sigma^2$. The output y at t+T will be same as in (37), thus its corresponding pdf and initial LLR can be defined as

$$f(y/x,\beta)=\frac{1}{\sqrt{2\pi\beta\sigma^2}}e^{\frac{-(y-\beta x)^2}{2\beta\sigma^2}} \quad (38)$$

$$L_{d\to h}^{0,0}(b_i)=\ln\frac{p(y/x=1,\beta)}{p(y/x=-1,\phi)}=\frac{2}{\sigma^2}y \quad (39)$$

Initial LLR mentioned above is a Gaussian random variable with mean $\frac{2\beta}{\sigma^2}$ and variance $\frac{4\beta}{\sigma^2}$. Further, we can write β as $\beta=\sum_{i=1}^{8}X_i$ .If we put m=8 in (35) then pdf of β can be expressed as $f(\beta)=\frac{1}{6}\beta^3e^{-\beta}$. Thus Final pdf of Initial LLR can be written as

$$f_{d\to h}^{0,0}(x)=\int_0^\infty\frac{1}{\sqrt{2\pi\left(4\beta/\sigma^2\right)}}e^{\frac{-\left(x-2\beta/\sigma^2\right)^2}{8\beta/\sigma^2}}.\frac{1}{6}\beta^3e^{-\beta}d\beta \quad (40)$$

Thereafter, we compute the pdf of LLR's after p inner and q outer iterations using (29) and (30).

5 Simulation Results

In this section, simulation results are shown for Alamouti coded LDPC-MIMO-OFDM systems under Rayleigh i.i.d channels. Firstly, the list of simulation parameters is shown in Table 3. These parameters are used for simulation of Fig. 1, and Fig. 3. For simulation purpose, (3, 6) regular LDPC code of rate 1/2 is used. It consists of 10 variable and 5 check nodes as shown in Fig. 4.

In regular LDPC codes, all nodes of same type will have same degree like in Fig. 4, all variable nodes are of degree 3 and check nodes of degree 6. For irregular codes degrees of each set of nodes are chosen according to optimized distribution. The optimized distribution for irregular LDPC codes under spatially uncorrelated MIMO-OFDM systems used in this paper is given by [26].

Table 3. Simulation parameters

Parameters	Values
Total Bandwidth	8MHz
Number of Transmit Antenna	2
Number of Receiving Antenna	2
FFT Size	4×1024
Carrier Modulation Used	QPSK
Guard period type	cyclic extension
Cyclic prefix length	1024
Window type	No windowing used
Channel Coding	Regular and Irregular LDPC codes
LDPC Code Rate	1/2
Number of Iterations	3000
Number of '1's Per Column (s)	3
Number of '1's Per Row (t)	6
Channel Model Used	Rayleigh i.i.d DVB-NGH Outdoor
Channel Fading	Rayleigh Independent and Identically distributed
Number of Channel Taps	8
Path Delays (in μsec)	0.02, 0.1094, 0.2188, 0.6094, 1.109,2.109,4.109,8.109
Channel Estimation	Ideal
Doppler Shift	33.3Hz

$$\lambda(x) = 0.269052x + 0.135031x^2 + 0.024564x^4 + 0.028685x^5 + 0.075819x^6 + 0.033661x^7 + 0.024360x^8 + 0.020951x^9 + 0.018975x^{10} + 0.014373x^{12} + 0.035585x^{13} + 0.015569x^{14} + 0.013611x^{16} + 0.289765x^{19} \quad (41)$$

$$\rho(x) = 0.307710x^7 + 0.692290x^8 \quad (42)$$

To support analytical results, simulation results are plotted, which shows variation of BER with respect to increase in signal to noise ratio (SNR). Results are obtained for both MIMO and MIMIO-OFDM system configurations.

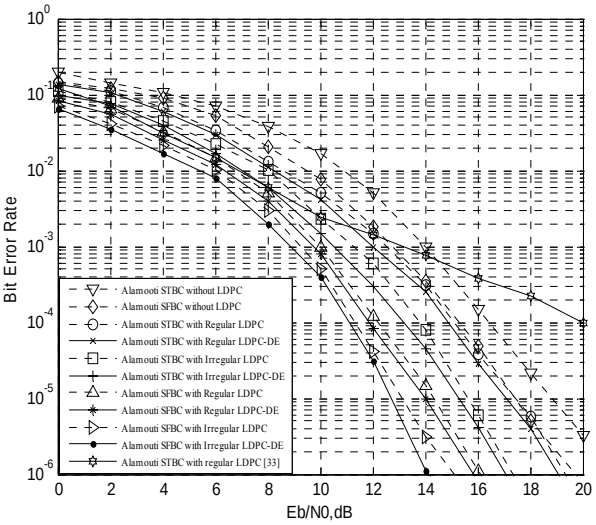

Fig. 5 BER performance of regular and irregular LDPC codes for 2×1 MIMO systems

Fig. 5, and 6 shows BER performance of 2×1 and 2×2 MIMO systems with and without LDPC codes.

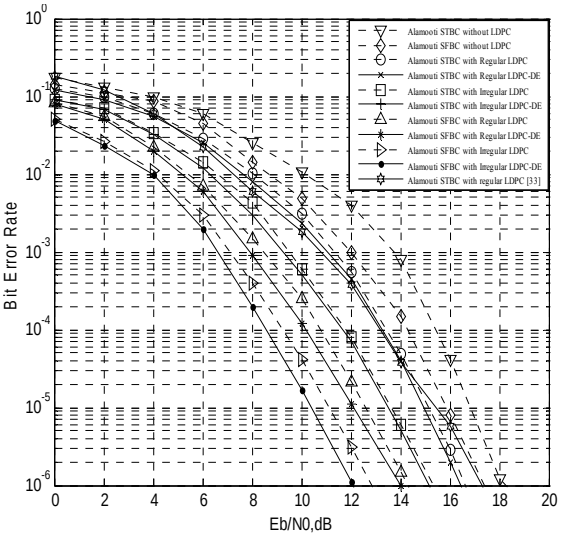

Fig. 6 BER performance of regular and irregular LDPC codes for 2×2 MIMO systems

Fig. 5, and 6 consists of 11 different cases, first 2 cases corresponds to Alamouti STBC and SFBC without LDPC, then next 8 cases corresponds to

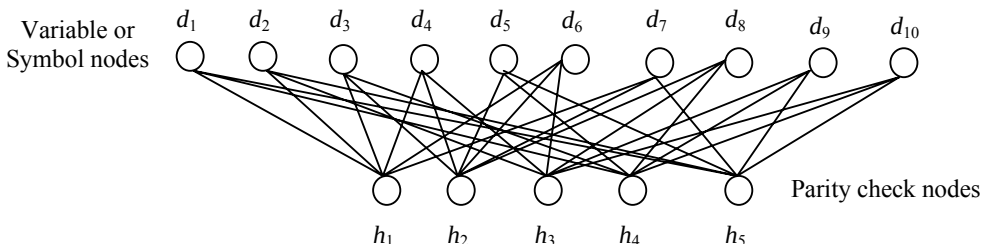

Fig 4, Bipartite graph for (3, 6) regular LDPC codes

Alamouti STBC and SFBC with regular and irregular LDPC codes along with results computed from DE analysis as mentioned in (28). The results of codes used in this paper are also compared with best available results in literature as shown by [33]. Fig.5,and 6 shows that BER is monotonically decreasing function of SNR. In Fig.5, BER decreases up to 3.2×10^{-6}at around 20dB in first case and then around 5.8×10^{-6} at 18dB, 5×10^{-6} at 18dB (simulated and DE), 6.1×10^{-6}at 16dB (simulated and DE), 1.5×10^{-5}at 14dB (simulated and DE) and 3.1×10^{-6} at 14dB (Simulated and DE) in subsequent cases. Similarly in Fig. 6, BER decreases up to 1×10^{-6} at around 18dB in first case and around 1×10^{-5}around 16dB, 2.8×10^{-6}around16dB (simulated and DE), 5.1×10^{-6} around 14dB (simulated and DE), 1.5×10^{-6}around 14dB (simulated and DE) and3.1×10^{-6}at 12dB (simulated and DE) in subsequent cases. The results in Fig. 5, clearly depicted that Alamouti SFBC with irregular LDPC outperforms remaining combinations due to its coding gain advantage and it also outperforms results from [33]. The result of Fig. 6, follows the same pattern as of Fig. 5. On comparing results of Fig. 5, with Fig. 6, it can be concluded that slope of BER curve is higher in Fig. 6, due to its higher diversity order. Further, SNR_{min-op} values calculated from Fig. 5, and Fig. 6, are tabulated in Table 4.

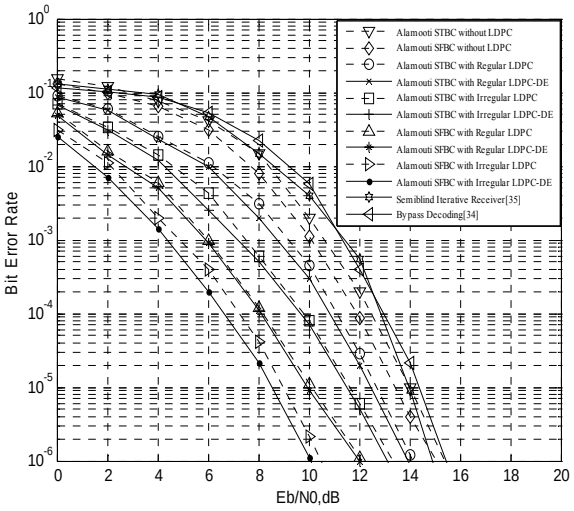

Fig. 7 BER performance of regular and irregular LDPC codes for 2×1 MIMO-OFDM systems

Fig. 7, and 8 shows results with 2×1 and 2×2 MIMO-OFDM systems. Results in both Figures are of same pattern as of Fig. 5, and 6. Results are also compared with best available codes in [34] and [35]. Among all combination of codes in Figs. 5-8, error rate performance of Alamouti SFBC with irregular LDPC in 2×2 MIMO-OFDM system is best due to its large coding gain and high diversity. Moreover, it also exhibit better mitigation to fading due to combination with OFDM. SNR_{min-op} values corresponding to Fig. 7, and Fig. 8, are shown in Table 4.

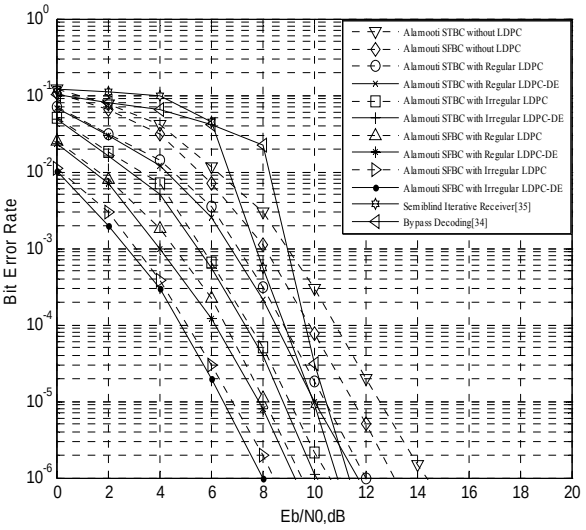

Fig. 8 BER of regular and irregular LDPC codes for 2×2 MIMO-OFDM systems

Table 4. SNR_{min-op} (in dB) values for various code combinations and system configurations

Parameter	MIMO		MIMO-OFDM	
Antennas → / Codes ↓	M_T=2, M_R=1	M_T=2, M_R=2	M_T=2, M_R=1	M_T=2, M_R=2
Reg-LDPC-STBC	8	7	5	3
Irreg.LDPC-STBC	6	5	3	2
Reg-LDPC-SFBC	5	4	1.8	0.4
Irreg.LDPC-SFBC	4	3	0.8	-2

Table 4, shows that Irregular LDPC codes along with Alamouti SFBC under 2×2 MIMO-OFDM system exhibits minimum value of SNR_{min-op}.

6 Conclusion

In this paper, we considered the performance analysis of serially concatenated regular and irregular LDPC codes with Alamouti STBC and SFBC MIMO-OFDM systems for high data rate wireless transmission. The DE tools based on pdf approach have been used for analyzing and

optimizing LDPC codes. It is also used to compute probability of error and minimum operational SNR required for DVB-NGH standard. We have evaluated BER results of irregular and regular LDPC codes with Alamouti STBC and SFBC under MIMO and MIMO-OFDM system configurations. From simulation results, we showed that optimized irregular LDPC codes concatenated with Alamouti SFBC in 2×2 MIMO-OFDM systems achieved best BER results. Comparing the results with existing results, it can be concluded that above mentioned combination will outperform the existing schemes in terms of complexity and minimum operational SNR. Further the simulation results and results obtained from DE analysis are almost identical. Work can be extended to increase the system reliability and reduce the decoder complexity.

References:

[1] D. Murch and K. B. Letaief, Antenna systems for broadband wireless access, *IEEE Communication Magazine*, Vol.40, No.4. 2002, pp. 76–83.

[2] H.Bolcskei, MIMO-OFDM wireless systems: basics, perspectives and challenges, *IEEE Wireless Communications,* Vol.13, No.4, 2006, pp. 31–37.

[3] D.S Saini and V. Balyan, OVSF code slots sharing and reduction in call blocking for 3G and beyond WCDMA networks, *WSEAS Trans On Communications,* Vol.11, No.4, 2012, pp. 135-146.

[4] N. Sharma and D. S. Saini, Code scattering and reduction in OVSF code blocking for 3G and beyond mobile communication systems, *WSEAS Transactions On Communications,* Vol.11, No.2, 2012, pp. 91-101.

[5] V. Tarokh, N. Seshadri, and A. R. Calderbank, Space-Time codes for high data rate wireless communication: performance criterion and code construction, *IEEE Transactions On Information Theory,* Vol.44, No.2, 1998, pp. 744–765.

[6] S. M. Alamouti, A simple transmit diversity technique for wireless communications, *IEEE Journal Of Selected Areas in Communications,* Vol.16, No. 8, 1998, pp. 1451–1458.

[7] W. Su and X. G. Xia, Signal constellations for Quasi-Orthogonal Space–Time Block Codes with full diversity, *IEEE Transactions On Information Theory,* Vol.50, No.10, 2004, pp. 2331–2347, 2004.

[8] W. Su, Z. Safar, and K. J. R. Liu, Full-rate full-diversity Space-Frequency codes with optimum coding advantage, *IEEE Transactions On Information Theory,* Vol.51, No.1, 2005, pp. 229-249.

[9] B. Gupta, and D. S. Saini, Space-Time/Space-Frequency/Space-Time-Frequency block coded MIMO-OFDM system with equalizers in quasi static mobile radio channels using higher tap order, Wireless Personal Communication, 2012, doi: 10.1007/s11277-012-0672-9.

[10] Z. Liu, Y. Xin, and G. Giannakis, Space-Time-Frequency coded OFDM over frequency selective fading channels, *IEEE Transactions On Signal Processing,* Vol.50, No.10, 2002, pp. 2465– 2476.

[11] W. Su, Z. Safar, and K. J. R. Liu, Towards maximum achievable diversity in space, time and frequency: performance analysis and code design, *IEEE Transactions On Wireless Communications,* Vol.4, No.4, 2005, pp. 1847-1857.

[12] M. Shahabinejad and S. Talebi, Full-diversity Space-Time-Frequency coding with very low complexity for the ML decoder, *IEEE Communications Letters,* Vol.16, No.5, 2012, pp. 658-661.

[13] W. Zhang, X. G. Xia, and P.C. Ching, High rate full diversity Space Time Frequency codes for broadband MIMO block fading channels, *IEEE Transactions On communications,* Vol.55, No.1, 2007, pp. 25-34.

[14] B. Gupta, and D. S. Saini, BER performance improvement in OFDM systems using equalization algorithms, in proc. *2010 1st International Conference on Parallel Distributed and Grid Computing (PDGC),* 2010, pp.49-54.

[15] R.Nordin, Interference-Aware Subcarrier Allocation in a Correlated MIMO Downlink Transmission, *WSEAS Transactions On Communications*, Vol.11, No.4, 2012, pp. 158-169.

[16] B. Gupta, and D.S Saini, A low complexity decoding scheme of STFBC MIMO-OFDM system, in proc. *Wireless Advanced (WiAd),* 2012, pp.176-180.

[17] C. Zheng, X. Chu, J. McAllister, and R. Woods, Real-valued fixed-complexity sphere decoder for high dimensional QAM-MIMO systems, *IEEE Transactions On Signal Processing*, Vol.59, No.9, 2011, pp. 4493-4499.

[18] S.M Tseng, Y.T. Hsu, and Y.R. Peng, Iterative multicarrier detector and LDPC decoder for OFDM Systems, *WSEAS Transactions On Communications*, Vol.11, No.3, 2012, pp. 124-134.

[19] R. Deepa and K, Baskaran, Analysis of subcarrier and antenna power allocation for MIMO WPMCM system with sphere decoder, *WSEAS Transactions On Communications*, Vol.11, No.3, 2012, pp. 113-123.

[20] H. Zhang, D. Yuan, and H. H. Chen, On array processing based Quasi-Orthogonal Space Time Block Coded OFDM systems, *IEEE Transactions On Vehicular Technology,* Vol.59, No.1, 2010, pp. 508-513.

[21] B. Gupta and D.S. Saini, BER analysis of ST-Block coded MIMO-OFDM systems with frequency domain equalization in quasi-static mobile channels, *Proc. India Conference (INDICON)2011 Annual IEEE),* 2011, pp. 1-4.

[22] H. Shah, A. Hedayat, and A. Nosratinia, Performance of concatenated channel codes and Orthogonal Space-Time Block Codes, *IEEE Transactions On Wireless Communications*, Vol.5, No.6, 2006, pp. 1406-1414.

[23] M.R. Islam and S.I. Ali, Encoding schemes for memory efficient quasi cyclic Low Density Parity Check Codes, *WSEAS Transactions On Communications*, Vol.11, No.6, 2012, pp. 218-23.

[24] D. J. C. MacKay and R. M. Neal, Near Shannon limit performance of Low Density Parity Check Codes, *Electronics Letters*, Vol.32, No.18, 1996, pp. 1645–1646.

[25] T. J. Richardson, M. A. Shokrollahi, and R. L. Urbanke, Design of capacity-approaching irregular Low-Density Parity-Check Codes, *IEEE Transactions On Information Theory*, Vol.47, No.2, 2001, pp. 619–637.

[26] B. Lu, G. Yue, and X. Wang, Performance analysis and design optimization of LDPC-Coded MIMO OFDM systems, *IEEE Transactions On Signal Processing*, Vol.52, No.2, 2004, pp. 348-361.

[27] B Lu, X. Wang, and K. R. Narayanan, LDPC based Space–Time Coded OFDM systems over correlated fading channels: performance analysis and receiver design, *IEEE Transactions On Communications*, Vol.50, No.1, 2002, pp. 74-88.

[28] H. E. Gamal, and A. R. Hammons, Analyzing the Turbo decoder using the Gaussian assumption, *IEEE Transactions On Information Theory,* Vol.47, No.2, 2001, pp. 671–686.

[29] S. Brink, Convergence of iterative decoding, *Electronics Letters*, Vol.35, No.10, 1999, pp. 1117–1118.

[30] Peter Moss et. al, DVB-NGH Channel Models, DVB-NGH document, 2010, pp. 1-13.

[31] L. M. Tanner, A recursive approach to low complexity codes, *IEEE Transactions On Information Theory,* Vol.27, No.5, 1981, pp. 533–547, 1981.

[32] T. J. Richardson and R. L. Urbanke, Capacity of Low Density Parity Check Codes under message passing decoding, *IEEE Transactions On Information Theory,* Vol.47, No.2, 2001, pp. 599–618.

[33]] J. Zhang and H. N. Lee, Performance analysis on LDPC coded systems over Quasi-Static (MIMO) fading channels, *IEEE Transactions On Communications,* Vol.56, No.12, 2008, pp. 2080-2093.

[34] Y. Xin, S. A. Mujtaba, T. Zhang, and J. Jiang, Bypass decoding: a reduced-complexity decoding technique for LDPC coded MIMO-OFDM systems, *IEEE Transactions On Vehicular Technology,* Vol.57, No.4, 2008, pp. 2319-2333.

[35] K. J. Kim, T. A. Tsiftsis, and R. Schober, Semiblind iterative receiver for coded MIMO-OFDM systems, *IEEE Transactions On Vehicular Technology,* Vol.60, No.7, 2011, pp. 3156-3168.

[36] A. Ohhashi and T. Ohtsuki, Performance analysis and code design of Low-Density Parity-Check (LDPC) coded Space-Time Transmit Diversity (STTD) system, in Proc: GLOBECOM'04 conference, 2004, pp. 3118-3122.